LHCb 2000-088 RICH
September 5, 2000

# Study of Multi Anode Photo Multiplier Tubes at Low Gains

S. Eisenhardt, F. Muheim[1]
University of Edinburgh
J .Bibby, J. Libby
University of Oxford

**Abstract**

We describe a preliminary study of the signal shape of the Multianode Photo Multiplier Tubes (MaPMT) at low gain. We investigate the feasibility of running the MaPMT at gains of around 30000 $e$ which would allow to use front-end chips that have been developed for silicon detectors or micro strip gas chambers. In addition we have investigated the focusing properties of an improved design of the MaPMT.

[1]Corresponding author. Email: F.Muheim@ed.ac.uk

# 1 Introduction

Multianode Photomultiplier Tubes (MaPMT) are being used as photo sensitive devices for large area Ring Imaging Cherenkov (RICH) detectors. For the LHCb experiment [1, 2] we have studied the performance of the MAPMT as a photo detector. The results from a series of tests carried out in 1999 with light emitting diodes (LED) and beam particles as sources of photons are described in a separate paper [3]. Earlier measurements can be found in References [4, 5, 6, 7].

An outstanding issue from these results is the optimization of the front-end electronics for the MaPMT as is reported in the MaPMT proposal [8]. We want to use ASIC front-end chips which have been developed for silicon detectors or Micro Strip Gas Chambers (MSGCs) which produce signals that are approximately 10 times smaller than those from the MaPMT. Therefore the MaPMT signals have to be attenuated to the dynamic range of the front-end chip. For the results reported in [3] we used an AC-coupler which was made with gold tracks laid on a ceramic base for this purpose. The front-end chip used was the APVm ASIC [9]. In this paper we describe a study of the signal shape of the MaPMT for different gains of the tube. By changing the ratios of the resistors of the dynode chains we investigate the feasibility of running the tube at lower gains of around 30000 $e$ which would allow us to use the available front-end chips without a need for either a separate attenuator or a redesign of the chosen chip. In addition we also present results comparing the tubes used in 1999 with a MaPMT with improved focusing made available to us by the manufacturer.

# 2 Multianode Photomultiplier Tubes

The multianode photomultiplier tube (MaPMT) consists of an array of square anodes each with its own metal dynode chain incorporated into a single vacuum tube to amplify the photoelectrons. The densest pixelization available, $8 \times 8$ pixels, provides the spatial resolution required for the LHCb RICH detector. The dynode structure is separated into 64 square pixels of 2.0 x 2.0 mm$^2$ area, separated by 0.3 mm gaps.

The 64-pixel MaPMTs are manufactured by Hamamatsu. The MaPMT R7600-03-M64, described in this paper has a 0.8 mm thick UV-glass window with a semi-transparent photocathode deposited on the inside. The threshold for the light transmission through the UV-glass window is at a wavelength of 200 nm. The photons are converted into photoelectrons in a Bialkali photocathode. For each pixel the photoelectrons are focused onto a 12-stage dynode chain and multiplied through secondary emission. The mean gain of the MaPMT is about $3 \times 10^5$ when operated at a voltage of 800 V. For the test carried out in 1999 and described in [3], nine MaPMTs have been purchased, preselected such that the average gain of the tubes varies not more than a factor of two.

Since then Hamamatsu has improved the quantum efficiency and the focusing properties of the MaPMT. Two tubes with these improvements were given to us on loan in January 2000. The quantum efficiency of the MaPMT, measured by Hamamatsu, is plotted versus the wavelength of the photons in Figure 2. Whereas the quantum efficiency of the nine tubes has a maximum of 22% at 380 nm the two new tubes have a maximum of 27% and 25% at 360 nm, respectively. Hamamatsu

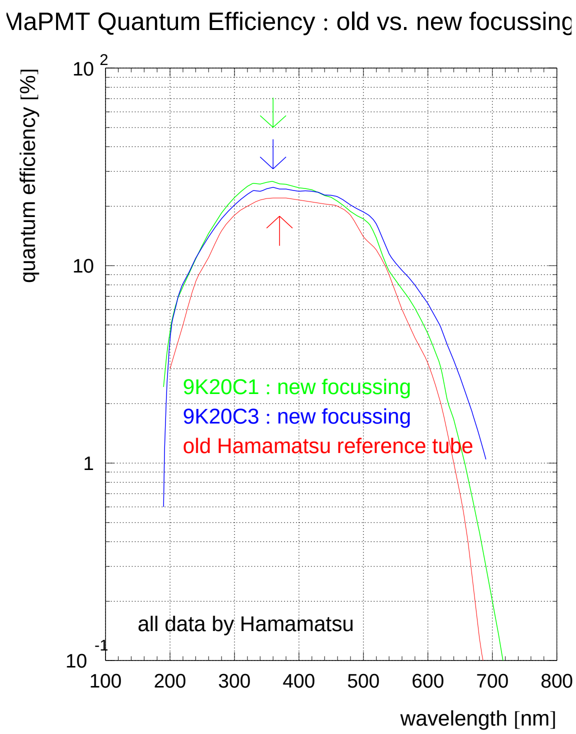


Figure 1: Quantum efficiency of the MaPMT R7600-03-M64 as a function of wavelength, measured by Hamamatsu.

also has improved the focusing of the photo electrons onto the entrance window. In Figure 2 we sketch the focusing schemes of the two new tubes and the nine old ones. The main differences are additional focusing wires and a wider entry area at the edge of the acceptance of the tube plus a reduction of the distance between focusing grid and entry slits.

To study the tubes at reduced gains the ratio of the resistors in the dynode chain has been varied. The main idea is to keep the voltage at the first few dynodes which mainly determines the signal shape and to reduce the gain of the later stages. In Table 2 we give the resistor values for three different sets of resistors chains between the dynodes. The three sets are different only in the values of $R$ for the resistors in front of the first three dynodes. The default resistor chain has been used for all other measurements presented here.

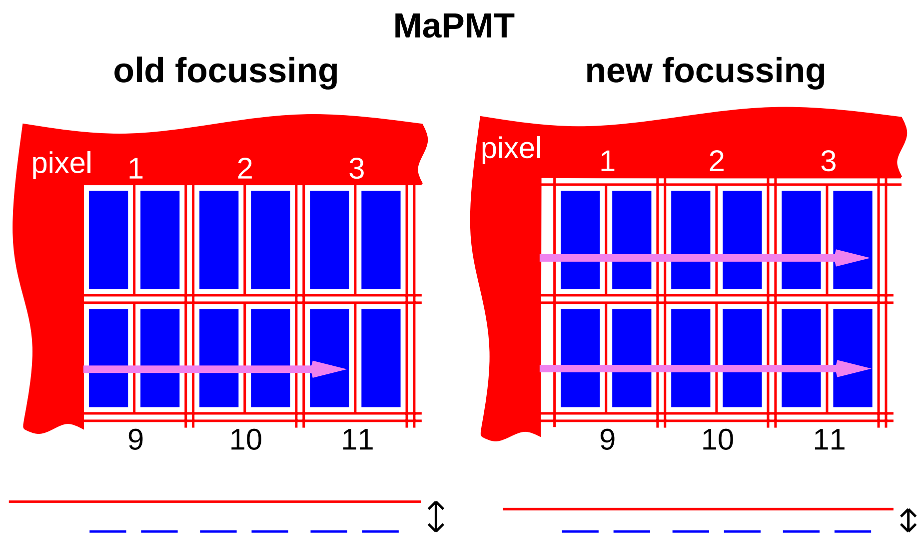


Figure 2: The focusing of the two new tubes versus the nine tubes purchased in 1999. There are additional focusing wires and a reduced distance between the new focusing grid and the dynode entry slits in the new tubes.

| Dynode | 1 | 2 | 3 | 4 | 5 | 6 | 7 | 8 | 9 | 10 | 11 | 12 | Anode |
|---|---|---|---|---|---|---|---|---|---|---|---|---|---|
| Default | 3 | 2 | 2 | 1 | 1 | 1 | 1 | 1 | 1 | 1 | 1 | 2 | 5 |
| Medium gain | 4 | 2 | 2 | 1 | 1 | 1 | 1 | 1 | 1 | 1 | 1 | 2 | 5 |
| Low gain | 4 | 3 | 3 | 1 | 1 | 1 | 1 | 1 | 1 | 1 | 1 | 2 | 5 |

Table 1: Resistances $R$ in $[10^5\ \mathrm{k}\Omega]$ in front of each dynode.

# 3 LED Scans

The response of the multianode photomultiplier tubes to single photons has been studied in the laboratory. The scanning facility is shown schematically in Figure 3. The light from a LED source that is coupled into a mono-mode fibre. A light beam with a width of about 100 $\mu$m and low emittance on the MaPMT surface is achieved with a gradient index lens and a small air gap. The tubes and the fibre are mounted on movable optical stages to allow scanning in the $x-$ and $y-$ direction. Using CAMAC electronics the signals from the tubes are amplified by a factor of 100 with 2 amplifiers in series and digitized by an ADC which is then read out by a computer. The trigger rate of the data acquisition system is about 1000 Hz.

The response of the MaPMT to single photons has been measured with this setup. The cathode voltage of the tube was set at -900 V. The LED voltage was set such that for about 30 % of the events at least one photon electron is produced at the photocathode within the timing gate of 200 ns. In Figure 4 we show a pulse height spectrum of a pixel of one of the new tubes. The broad signal containing mostly one photo electron and the pedestal peak are clearly visible. The mean pulse

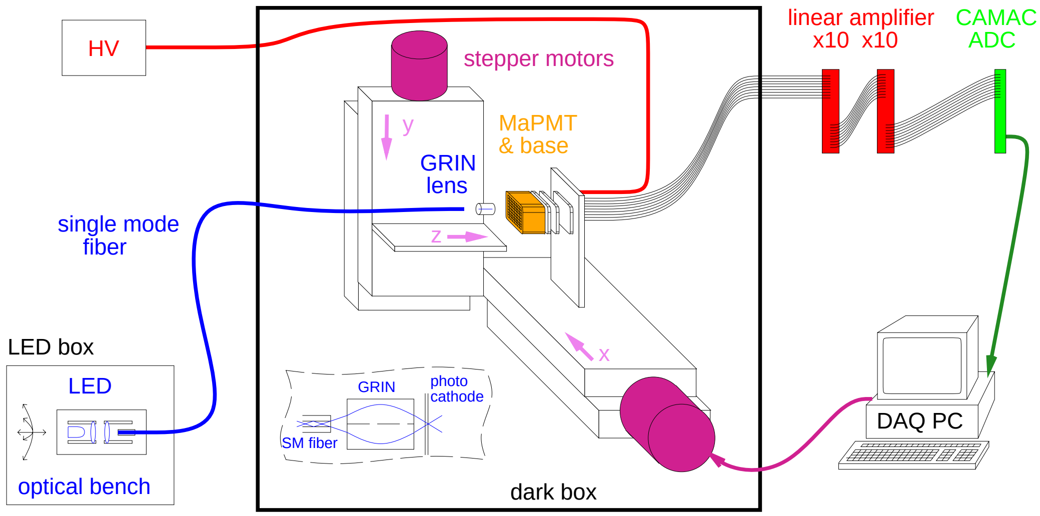


Figure 3: The MaPMT scanning facility

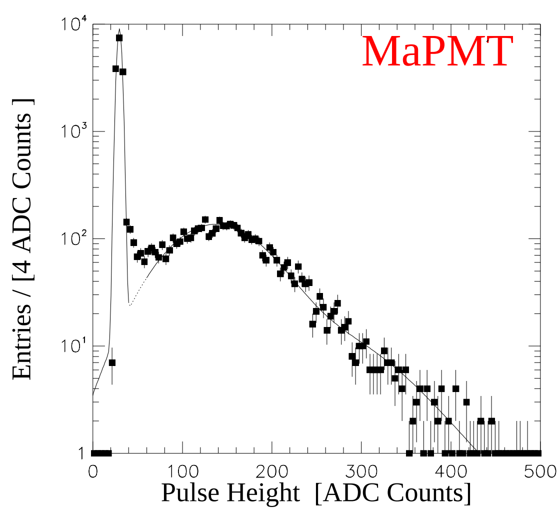


Figure 4: Single photon spectrum of MAPMT pixel.

height is at around 100 ADC counts above pedestals. The spectrum has been fitted by a function which allows a Gaussian shape for each photo electron signal and for the pedestal peak. The number of photo electrons $n_{pe}$ in an event has to follow a Poisson distribution. The sigma of the Gaussian signal shapes are constrained to be proportional to $\sqrt{n_{pe}}$. The fit is superimposed on the data points. The sigma of the single photon signal is about 50 ADC counts. The signal to pedestal width ratio is 40:1.

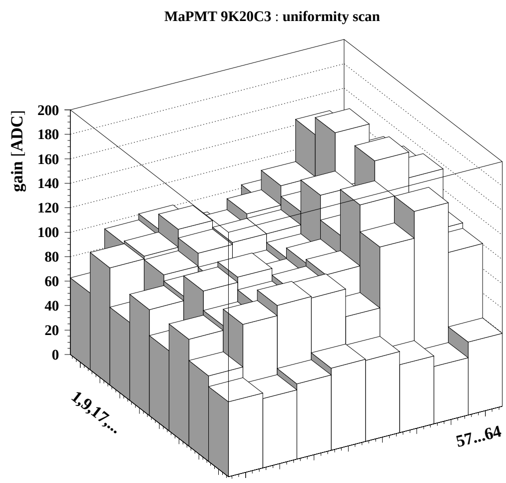


Figure 5: Mean pulse height of all 64 channels of an MaPMT.

The gain varies for the 64 different dynode chains within a tube. In Figure 5 we show the mean pulse height of all 64 channels of the new tube. The gain variations are about a factor of two with an RMS spread of about 30 % about the mean value. The gain is lower for the edge columns. This has been investigated in more detail by scanning across the tubes in steps of 0.1 mm. We present a comparison of edge effects for the new tube with respect to one of the nine tubes that have been used for the test beam. The measured gain as a function of the position of the light source across the tube is shown in the top of Figure 6. The solid and dashed lines correspond to new and old focusing, respectively. The gain of the tubes with the old focusing is clearly inhomogeneous for the edge pixel and drops before the geometrical edge of the pixel. With the new focusing the gain profile for the edge pixel is similar to that of the other pixels. This improvement is also reflected in the measurement of the average number of observed photons, $\lambda$, as shown in the bottom of Figure 6. The collection efficiency of the MaPMT, which is proportional to $\lambda$, is clearly improved by the new focusing.

We now present the preliminary results of the signal shape of the MaPMT at different gains. On the left of Figure 7 we plot the measured pulse height using the low gain resistor chain (see Table 2) with the photo cathode set at -900 V. The mean single photon signal is now at about 20 ADC counts above the pedestal

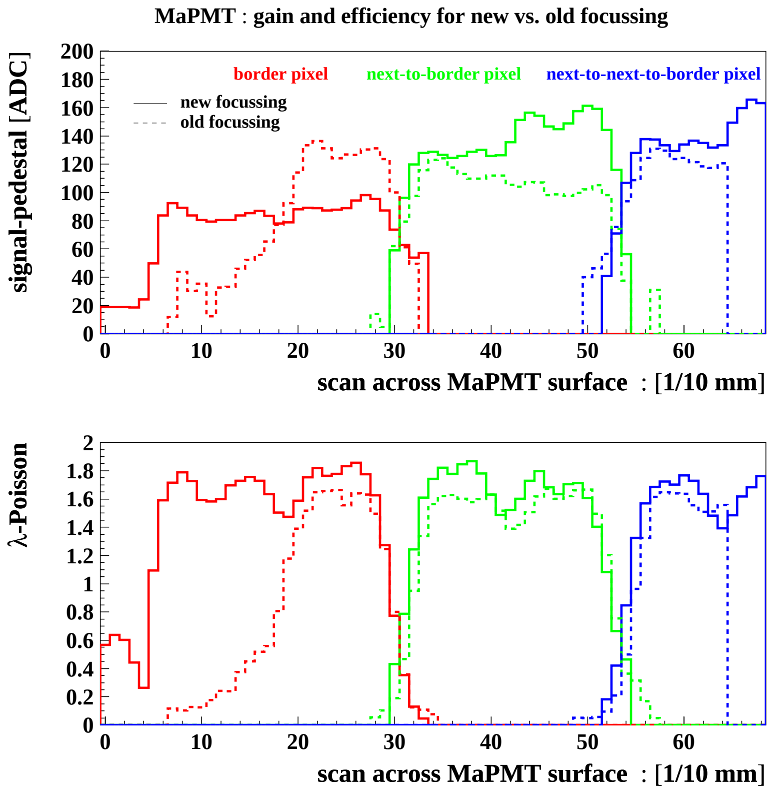


Figure 6: Scan across an MaPMT.

which is clearly smaller than for the default resistor chain (Figure 4). The mean signal to pedestal width ratio is reduced to 7. This is at the edge of the sensitivity of the electronics chain. The gain of the MAPMT becomes larger with increasing negative high voltage applied to the photocathode. This is illustrated in Figure 7 where we plot the measured pulse height spectrum for the low gain resistor chain at a cathode voltage of -900 V and -960 V, respectively. The signal size increases by about a factor of 2.5. We have recorded the pulse height spectra with the three different sets of resistors chains between the dynodes for cathode voltage between -700 V and -1000 V (high voltage scan). In Figure 8 (top) we plot the measurements of the mean pulse height after pedestal subtraction for an inner and a border pixel versus the high voltage at the photocathode. This shows that the gain increases exponentially and doubles when increasing the voltage by about 50 V. This variation is quite independent of the actual gain, i.e the same for the different dynode resistor chains. On average the gain for the low gain resistor chain is 3.9 times smaller than for the default ratios.

To be able to run the MaPMT at lower gains we also need to study the shape of the pulse height spectrum. Ultimately we need to know the loss of signal due to two effects: Firstly for a given threshold requirement, e.g. the signal must be higher

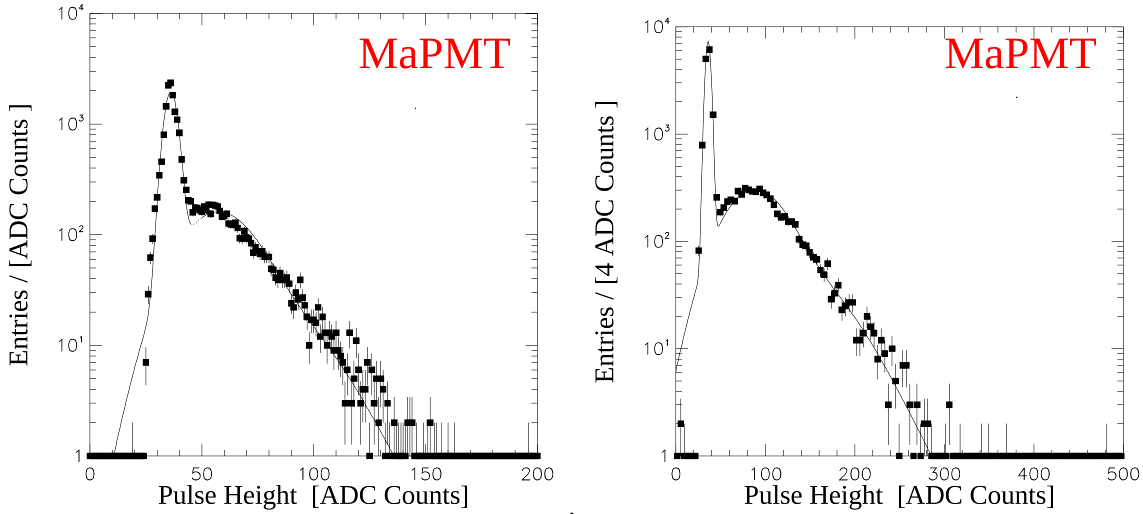


,

Figure 7: Pulse height spectrum of the MAPMT with the low gain resistor chain. The cathode voltage is -900 V (left side) and -960 V (right side), respectively.

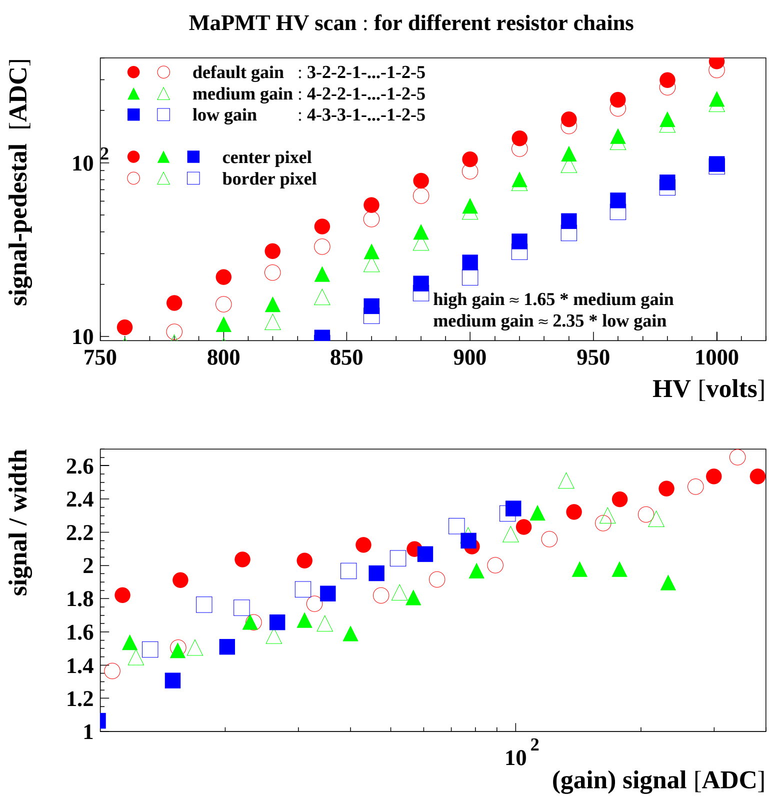


Figure 8: High voltage scan for 3 different resistor chains. Top plot is signal vs high voltage at the photo cathode and bottom plot is signal/width vs signal.

than 5 times the sigma of the pedestal, photo electrons are lost if their amplitude is below this cut-off. Secondly, there is a Poissonian chance of no multiplication at the dynode stages. This effect occurs mainly at the first dynode thus its rate depends on the gain at the first dynode $g_1$. The ratio of single photon signal $s$ to its Gaussian width $\sigma$ allows us to estimate a lower limit for the gain at the first dynode $g_1 > (s/\sigma)^2$. In Figure 8 (bottom) we plot the ratio $s/\sigma$ as a function of $s$ for the high voltage scan. The data points for the three different resistor chains are overlayed. The data show as expected that $s/\sigma$ increases with increasing high voltage. At a given gain the low gain (blue squares) data points are a little lower that the default dynode chain (red circles) data points. However this difference is comparable to the spread between the two pixels, i.e. solid versus open data points. No quantitative analysis of the signal loss has been made[2]. At a photo cathode voltage of -900 V the loss due to no multiplication at the first dynode which is equal to $\exp -g_1$, is smaller than 2.5%. The data points with small signals ($s < 25$) have mean signal over pedestal width ratios smaller than 10. In this range additional uncertainties are present in the extraction of the signal shape parameters $s$ and $\sigma$ due to the limited separation between signal and pedestal peak.

# 4 Conclusion

We have evaluated the focusing properties of two new MaPMTs. The collection efficiency of these tubes is clearly improved by the new focusing. We have also performed a peliminary study of the MaPMT using different dynode resistor chains. At a given voltage we have achieved a gain reduction of a factor of four. A reduction of a factor of ten can be obtained with the low gain resistor chain when lowering the voltage at the photo cathode by about 50 V. However an accurate measurement of the signal shape in this range is beyond the sensitivity of the electronics used for this measurement. The data show that at higher gains the width of the pulse height distribution is slightly larger for the low gain dynode chain. If confirmed this widening would increase the signal loss below a threshold cut. We conclude that the operation of the MaPMT at lower gains could be possible. However additional studies with a more sensitive electronics at these low gains are needed to obtain more quantitative results before we can make definite statement about the performance of the MaPMT at gains of 30000 $e$.

We plan to carry out more measurements using the APVm electronics chain [3, 9] with the following modification: The signals from the MaPMT will bypass the AC-coupler network thus the sensitivity of the APVm will be greatly increased and we should be able to run at gains of 30000 $e$.

[2]The data were lost due to a disk crash. The signal loss calculation will be added later.

## References


[1] "A Large Hadron Collider Beauty Experiment for Precision Measurements of CP Violation and Rare Decays"; LHCb Technical Proposal, LHCC 98/04, LHCC/P4 (Feb. 1998).

[2] The LHCb RICH detector web page: "http://lhcb.cern.ch/rich/".

[3] V. Gibson *et al.*, "Performance of a Multianode Photo Multiplier Cluster equipped with Lenses", LHCb 2000-083 RICH.

[4] A. Duane *et al.*, "Cherenkov Rings Detected with a Multianode P.M.T.", LHCb/98/039 RICH.

[5] N. Smale *et al.*, "Evaluation of the Multianode Photomultiplier for the LHCb RICH detectors", LHCb/98/066 RICH.

[6] E. Albrecht *et al.*, "Latest beam test results from RICH prototypes using hybrid photo detectors and multi anode PMTs", Nucl. Inst. Meth. **A 433** (1999) 159.

[7] E. Albrecht *et al.*, "A Prototype RICH Detector Using Multi-Anode Photo Multiplier Tubes and Hybrid Photo-Diodes", LHCb 2000-068 RICH, submitted to Nucl. Inst. Meth. **A**.

[8] F. Muheim, *et al.*, "Proposal for Multi-Anode Photo Multiplier Tubes as Photo Detectors for the LHCb RICH", LHCb 2000-065 RICH.

[9] M.D.M. de Fez-Laxo *et al.*, Nucl. Inst. Meth. **A 382** (1996) 533.
M. Raymond *et al.*, London 1997, "Electronics for LHC Experiments" CERN/LHCC/97-60 (1997) 158.// L.L. Jones *et al.*, Rome 1998, "Electronics for LHC Experiments" CERN/LHCC/98-36 (1998) 185.